HHS Public Access

Author manuscript

Environ Sci Technol. Author manuscript; available in PMC 2018 March 19.

Published in final edited form as:

Environ Sci Technol. 2017 September 19; 51(18): 10396–10402. doi:10.1021/acs.est.7b01521.

Effect of Particulate Matter Mineral Composition on Environmentally Persistent Free Radical (EPFR) Formation

Elisabeth E. Feld-Cook[†,‖], **Lisa Bovenkamp-Langlois**[‡,‖], and **Slawo M. Lomnicki**[§,*,‖]

[†]Department of Chemistry, Louisiana State University, Baton Rouge, Louisiana 70803, United States

[‡]Center for Advanced Microstructures & Devices (CAMD), Louisiana State University, Baton Rouge, Louisiana 70803, United States

[§]Department of Environmental Sciences, Louisiana State University, Baton Rouge, Louisiana 70803, United States

Abstract

Environmentally Persistent Free Radicals (EPFRs) are newly discovered, long-lived surface bound radicals that form on particulate matter and combustion borne particulates, such as fly ash. Human exposure to such particulates lead to translocation into the lungs and heart resulting in cardio-vascular and respiratory disease through the production of reactive oxygen species. Analysis of some waste incinerator fly ashes revealed a significant difference between their EPFR contents. Although EPFR formation occurs on the metal domains, these differences were correlated with the altering concentration of calcium and sulfur. To analyze these phenomena, surrogate fly ashes were synthesized to mimic the presence of their major mineral components, including metal oxides, calcium, and sulfur. The results of this study led to the conclusion that the presence of sulfates limits formation of EPFRs due to inhibition or poisoning of the transition metal active sites necessary for their formation. These findings provide a pathway toward understanding differences in EPFR presence on particulate matter and uncover the possibility of remediating EPFRs from incineration and hazardous waste sites.

Graphical Abstract

[*]Corresponding Author: slomni1@lsu.edu (S.M.L.).

‖Author Contributions

These authors contributed equally to this work. The manuscript was written through the contributions of all authors. All authors have given approval to the final version of the manuscript.

ORCID

Elisabeth E. Feld-Cook: 0000-0002-9308-9037

Notes

The authors declare no competing financial interest.

Supporting Information

The Supporting Information is available free of charge on the ACS Publications website at DOI: 10.1021/acs.est.7b01521.

XPS spectra of real world and surrogate fly ashes and XANES spectra of real world fly ashes and XANES reference spectra for S and Fe (PDF)

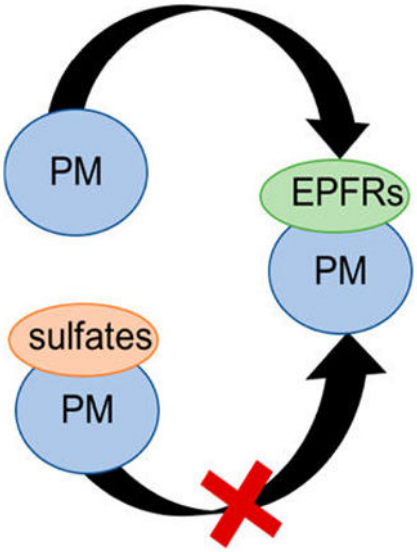

INTRODUCTION

Particulate emission from combustion systems is typically a carrier of many condensable pollutants including but not limited to heavy and transition metals, polycyclic aromatic hydrocarbons (PAHs), polychlorinated dibenzo-*p*-dioxins and dibenzofurans (PCDD/Fs), polybrominated dibenzo-*p*-dioxins and furans (PBDD/Fs), and other halogenated compounds. Particulate matter (PM) and fly ash (FA) are the largest transporters of these pollutants through the air. Within the last 10 years a new type of pollutant associated with PM has been discovered: Environmentally Persistent Free Radicals (EPFRs).

EPFRs are long-lived surface bound radicals known to form on particulate matter.[1] Their formation typically occurs in the cool zone of combustion systems, where the temperature drops below 600 °C,[2] through a series of surface mediated reactions[2–4] between transition metals (iron, copper, nickel, and zinc[5–7]) and organic precursors such as (but not limited to) chlorinated benzenes and phenols. The organic aromatic precursor adsorbs to the metal oxide on the surface of the particulate (Scheme 1).[1]

The lifetime of EPFRs in atmospheric conditions ranges from 1 to 5.2 days.[5–7] This extreme and unusual stability of such surface-bound radicals is currently not fully understood. However, it is believed to be a result of the following factors: the resonance between the carbon and oxygen centered radicals, metal center charge transfer, surface stabilization effects, and changing degrees of freedom.

EPFRs are a risk to human health through both acute[2,8–12] and chronic exposure.[11,13] Further, they are intermediates in the formation of polychlorinated dibenzo-*p*-dioxins and polychlorinated furans (PCDD/F).[14,15] The major route of human exposure is through PM inhalation; once in the lungs, EPFRs undergo a cyclic process with the net output of reactive oxygen species (ROS). The overproduction of ROS results in oxidative stress increasing susceptibility to respiratory and cardiovascular diseases.[1,4,12,13,16–21] The condensation

reactions that EPFRs undergo to form PCDD/Fs constitute another significant environmental and health risk that calls for EPFR prevention.

Recent EPFR studies have primarily focused on the mechanistic understanding of EPFR formation, fate, and properties on single metal-oxide systems.[1,14,22,23] While important, single-metal oxide systems are not an accurate depiction of real world combustion systems because many of the condensable pollutants (i.e., metals) are present at the EPFR inception conditions. Therefore, studying mixed metal-oxide complexes with additional components (i.e., calcium and sulfur) will give a more accurate representation of PM & FA produced during the incineration process. In the presented research study, we were particularly interested in whether EPFR formation can be affected by chemical activity of the PM surface composition in the cool zone of combustion systems.

To investigate the potential effects of the surface chemistry as well as calcium and sulfur presence on the formation of EPFRs, a set of model particles was constructed. The model composition was based on incinerator fly ash analysis with respect to their major inorganic elemental components and subjected to EPFR formation tests. A combinatorial bottom-up approach was taken with respect to introducing calcium and sulfur into the system, where both of the elements were either cointroduced or subsequently added into the surrogate ash, in both the solid formation and postformation stages. These two approaches correspond to different off-gas treatment methods, either in the postflame zone or cool zone.[2] In the postflame zone, all of the initial waste is atomized, and the particles start to condense; by adding the calcium and sulfur at this stage, it can change the particle chemistry and alter the chemical composition of solids. Alternatively, adding calcium and sulfur in the cool zone as a post-treatment agent, where EPFRs form, can potentially affect the surface chemistry of the formed particles.[24,25] In addition to the elemental composition determined by Inductively Coupled Plasma-Atomic Emission Spectroscopy (ICP-AES) and X-ray Fluorescence (XRF), different techniques were applied to characterize the atomic/molecular structure of the EPFRs in real-world and surrogate FA. The surface composition of the real-world and surrogate FA was examined using X-ray Photoelectron Spectroscopy (XPS). X-ray Absorption Near Edge Structure (XANES) spectroscopy was used to determine the chemical environment and coordination of sulfur and iron in both real world and surrogate FA within the bulk of the samples.

MATERIALS AND METHODS

Real World Fly Ashes

These samples were collected from bag houses from the United States Environmental Protection Agency medical waste incinerators (MEDWI) and from multiple municipal waste incineration sites (MWI) in the following eastern and southeastern cities of the People’s Republic of China: Bingjiang, Ding Hu, Ning Bo, Xiao Shan, and Yuhang. The samples were collected by local researchers and were used immediately upon receipt to minimize radical decay.

Surrogate Fly Ash Synthesis

Cabosil (Cabot, 99+%, specific surface area 380 m^2/gram, Cab-o-sil EH-5) was impregnated using the incipient wetness method[5] with metal nitrates in a water solution to obtain particles with final metal concentrations of 0.1% Cu, 5% Fe, 2% Mg, and 2% Zn (Table 1). Some ashes were additionally impregnated with calcium nitrate and/or ammonium sulfate to achieve final concentrations of 30% Ca and 10% S. The order of introduction of the elemental components to the surrogate fly ashes is presented in Table 1. In general, two types of fly ashes were synthesized: (I) with Ca and/or S introduced into the surrogate fly ashes together with metal components (before-calcination or B samples) and (II) with Ca and/or S introduced into the surrogate fly ashes in a second stage, once metal oxides were already formed (postcalcination or P samples).

Following the introduction of the precursors onto the matrix, surrogates were left to adsorb the components for 24 h. The surrogates were then dried in an oven for 12 h at 120 °C. Lastly, the surrogates were calcined for 5 h at 450 °C and sieved to the 60 mesh size. For B samples, ashes were impregnated simultaneously with metal nitrates, Ca, and/or S precursors using the incipient wetness method. For P samples, ashes went through the incipient wetness method twice, with the first time containing only metal nitrates and the second time with Ca and/or S precursors.

EPFR Formation on Surrogate Fly Ash

The procedure for EPFR formation was adapted from Dellinger et al. 2007.[3] In short, the ash surface, after initial activation under vacuum for 1 h at 450 °C, was exposed at 230 °C to 2-monochlorophenol (2-MCP, Aldrich 99%) vapors for 5 min.[3,6] Following the exposure, samples were evacuated for 1 h, cooled to room temperature, and the EPR measurement was taken by the procedure described in the next section.

Electron Paramagnetic Resonance (EPR)

EPFRs were measured on a Bruker EMX EPR 10/2.7 using the following parameters: 9.8 GHz, 2.0 mW power, centerfield 3460 G, time constant 40.96 ms and 3.56×10^4 gain. Collected spectra were the average of 3 scans. 2,2-Diphenyl-1-picrylhydrazyl (DPPH) was used as a standard for EPFR concentration calibration and calculation.[26] The EPFR concentration was calculated by directly comparing the radical concentration in the ashes to the standard, DPPH, and normalizing for experimental parameters. Radical species determination was based on the *g*-value, a mathematical parameter derived from the energy difference during the excitation and relaxation of the radical electron.

Inductively-Coupled Plasma-Atomic Emission Spectroscopy (ICP-AES)

Ashes were digested in a 1:1:3:5 mixture of HCl to HNO_3 to HF to H_2O using a CEM Microwave Accelerated Reaction System (MARS) 5 at 200 °C for 60 min. Spectra were taken on a PerkinElmer ICP-AES.

X-ray Photoelectron Spectroscopy (XPS)

All XPS experiments were performed on a Kratos Axis 165 Auger/XPS using a mono-Al beam. Ashes were pressed into pellets (~1 mm) and mounted on carbon tape. A single survey scan was taken over the range of 0–1200 eV, at 80 eV pass energy, with 0.5 eV step size and 100 ms dwell time. Individual elements were scanned twice over their specific energy range (based on the Binding Energy (BE) values from the NIST database) for a high-resolution scan at 40 eV pass energy, with 0.1 eV step and 100–500 ms dwell time.[27–30]

X-ray Absorption Near Edge Structure (XANES)

For XANES, sample preparation was similar to Hormes et al.[31] and analyzed at the Low Energy X-ray Absorbance Spectroscopy (LEXAS) beamline in fluorescence mode at the Center for Advanced Microstructures and Devices (CAMD) in Baton Rouge, LA. XANES measurements at S K-edge (2470 eV) were taken at a reduced pressure of 42 Torr inside the experimental setup over the following ranges and step sizes: pre-edge (2449–2469 eV, 1 eV), main edge (2069–2499 eV, 0.2 eV), and postedge (2499–2520 eV, 0.5 eV). Due to high sulfur content, the self-absorption correction in the ATHENA program was used before data analysis. XANES measurements at the Fe K-edge (7113 eV) were taken over the following ranges and step sizes: pre-edge (6913–7083 eV, 5 eV), main edge (7083–7143 eV, 0.5 eV), postedge 1 (7143–7213 eV, 1 eV), and postedge 2 (7213–7662 eV, 0.05k). Composition analysis was performed using ATHENA of the IFFEFIT[32] package to normalize, analyze, and perform linear combination fitting (LCF) of all spectra.[32,33]

RESULTS AND DISCUSSION

Real World Fly Ash Radical Composition Characterization

Previous studies of combustion derived samples such as diesel particulates, PM samples and different soot materials have indicated a ubiquitous presence of EPFRs.[14,25,26] In contrast to previous studies, a significant difference in radical concentration was detected for fly ashes collected at U.S. and China incineration facilities (Figure 1).

Samples collected at medical waste incinerators in the U.S. (MEDWI) have a radical concentration of 10^{17}spins/gram (Figure 1). The detected radicals are characterized by an average g value of 2.0028 and average $\Delta H_{p\text{-}p}$ of 3.567. The broad radical signal (>6 G) indicates the multicomponent makeup of the EPFRs present on these samples. These EPFRs are characteristic of primarily carbon-centered radicals based on the g-value and low $\Delta H_{p\text{-}p}$ values. The $\Delta H_{p\text{-}p}$ corresponds to the width between the peaks which gives insight into the number of radicals present in a sample.[34]

Contrary to MEDWI ashes, MWI ashes do not have a detectable radical concentration. This is unusual, as EPFRs have been commonly found in combustion-emitted particulates. One of the reasons for the lack of EPFRs in the MWI ashes could be an analytical artifact. The high concentration of paramagnetic metal species in the MWI ashes produced a very strong EPR signal, which caused tuning problems and required EPR measurements to be performed on ashes with a mass 10 times lower than normal. Lower sample mass may have caused the EPFR concentration to fall below the detection limit. Therefore, the EPFRs, while

potentially on the surface, are not detected by the EPR. Nevertheless, even in such an event, the overall concentration of EPFRs would be much smaller compared to other samples (1–2 orders of magnitude). Low concentrations of EPFRs (or complete absence) on MWI ashes provide an interesting opportunity to investigate the factors inhibiting their formation on the surface of the ashes.

Real World Fly Ash Elemental Composition Characterization

It is well documented that EPFRs are associated with the presence of transition metals, which act as the reaction/formation center and contribute to radical stabilization on the surface.[5–7,35] Previous studies have also shown that different metal speciations result in varying radical yields and changes to their persistency in ambient air.[14] Among the studied metals, copper and iron have shown the highest activity of EPFR formation, while zinc and nickel indicated extremely long EPFR lifetimes in ambient air (in months).[5–7,35] The elemental analysis of the bulk ashes by ICP-AES is presented in Table 2.

Distinct differences can be observed between the MWI and MEDWI samples: the major metal component on MWI ashes is Fe with 1–4%, while the Fe content of MEDWI ashes is only 0.2%. However, MEDWI contain higher quantities of Zn (4–6%) compared to MWI. Among other elements, sulfur shows distinctly higher concentrations in MWI ashes. Also, for the majority of MWI ashes, calcium is more abundant than for the MEDWI ashes.

It is important to understand the difference of the elemental composition between surface vs bulk of the ashes since EPFRs are surface bound radicals. If the metal sites responsible for EPFR formation were unavailable at the surface, then this could impact the observed differences in EPFR concentration in the real world fly ashes. The elemental composition of the surface for MEDWI and MWI investigated by XPS (Table 3 and SI Figure S1) further emphasizes the differences between these two types of ashes. The surface of MEDWI ashes contain significant amounts of carbon, which is expected for the combustion-borne particulates. MEDWI ashes also contain Zn both on the surface and in bulk (see ICP analysis above). For MWI ashes, no iron, copper or zinc was detected on the surface by XPS; however, high amounts of calcium and sulfur were observed (not detected at MEDWI surface). At the same time the carbon content on the surface was significantly reduced for MWI, compared to MEDWI. While the bulk elemental composition of fly ash samples can be related with the composition of waste burned, the enrichment of the surface with calcium and sulfur may be related to the post-treatment of the combustion exhaust. Limestone and lime injection at the high temperature zone of combustors is the cheapest and most common practice for SO_2 emission control[36,37] and results in the formation of calcium sulfate. XANES analysis of the MWI ashes has indeed confirmed that sulfur is mostly present in the form of sulfate on those samples (SI Figure S2).

The formation of large amounts of calcium sulfate can have a significant impact on the detected concentration of EPFRs on the samples. First, precipitation and deposition in the collection devices of large quantities of calcium sulfate will result in a “dilution effect” of combustion borne particulates—although the total output of fly ash and EPFRs would not be changed; introduction of calcium sulfate will decrease per unit mass concentration of EPFRs. Second, precipitating calcium sulfate can deposit on the surface of already formed

PM, blocking access to the surface metal centers, which are active down the exhaust stream in the formation of EPFRs. Third, introduction of large lime or limestone quantities indicates high concentrations of SO_2 in the systems—it is possible that SO_2 interacts with metal centers and prevents the formation of EPFRs. With that said, there is evidence to show that sulfur compounds have an effect on particulate formation from incineration processes. [38,39]

It is unclear which scenario is applicable to MWI ash, but the data may provide vital information on ways to control EPFR formation/emission from combustion sources. Indeed zinc, identified earlier as an EPFR active metal, is the prominent surface element in MEDWI ashes, which also contained EPFRs. The detection of a significant amount of iron deep in the bulk of MWI ash further suggests its inability to bind to the organics on the surface, therefore hindering EPFR formation (iron was not detected on the surface of those samples —Table 2).

Surrogate Fly Ash Radical Formation

To further investigate these effects, we have designed a set of model fly ash composed of the common metals present in the incinerator fly ashes and supplemented them with calcium and sulfur. The inclusion of Ca and S mimics their introduction in the postflame and cool zone of the incinerators: lime injections into combustion processes (dry or wet) and reactivity of gaseous SO_2 with the surface.

The introduction of just calcium ions to ashes, for both sample types, before and post calcination, did not significantly affect the EPFR formation as the mixed metal (MM) surrogates produced a similar concentration of EPFRs after exposure to the radical precursor (BMMCa and PMMCa—Figure 2). The addition of both calcium and sulfur to the metal bearing surrogate unexpectedly increased the propensity of the surrogates to generate EPFRs. While this result is unexpected, it is consistent with both BMMCaS and PMMCaS. However, it is beyond the scope of this study to understand the chemical nature of this phenomenon. In contrast to the rest of the surrogates, introduction of only sulfur to the surrogates strongly suppressed the ability for EPFRs to be formed on such surrogates. The EPFR concentration upon exposure to the radical precursor on BMMS and PMMS surrogates was lower by a factor of >100 when compared to BMMCa, PMMCa, and MM.

The effects of sulfur on the emission of organic pollutants have been previously reported. Studies have shown that PCDD/F emissions are suppressed by sulfates.[40] There is a close relationship between EPFR and PCDD/F emissions as EPFRs are direct intermediates to PCDD/Fs in their surface mediated formation in the cool zone of incinerators.[41–43] Considering the mechanism of EPFR formation, where the organic precursor chemisorbs on the metal site, one can speculate that the presence of sulfur dioxide can result in the adsorption of SO_2 on the metal centers forming surface sulfate species. Indeed, SO_2 is a known catalytic poison for metal oxide catalysts by surface sulfidation.[44,45]

To analyze the role of sulfur in EPFR suppression, XANES studies were performed at the S K-edge (Figure 3). The XANES spectra could not be analyzed by LCF due to the high disorder in the noncrystalline phase of the amorphous surrogates[46] which could not be represented by linear combinations of the available crystalline structure reference

compounds. Disorder is higher in amorphous materials and causes broadening of the peak shapes, i.e., shape resonances in the case of sulfur, used to distinguish between sulfate species. The S K-edge XANES spectra of BMMCaS and PMMCaS (Figure 3) show the following features: the sulfate white line maximum at 2481.4 eV, a postedge peak at 2485 eV, and shape resonances with maxima at 2492 and 2498 eV that are characteristic of the S K-edge XANES spectrum for anhydrite calcium sulfate (sulfur references are shown in SI Figure S4). On the contrary, the XANES spectra of BMMS and PMMS do not have a postedge peak at 2485 eV and only a very broad shape resonance with maxima at 2497 eV, indicating the absence of anhydrite calcium sulfate. The shape of this shape resonance has more similarity with zinc sulfate or iron sulfate. On the basis of the composition and S K-edge XANES spectra of BMMS and PMMS, iron and/or zinc sulfate are the most probable sulfate species present in these surrogates. Shape resonances resembling iron and/or zinc sulfate are not present in BMMCaS and PMMCaS, which indicates the potential availability of Fe and Zn ions to form EPFRs on those samples.

Iron sulfate formation on BMMS and PMMS surrogates was further confirmed using XANES studies at the iron K-edge (Figure 4, iron references shown in SI Figure S5). The dominant species determined using LCF analysis for BMMS and PMMS is iron(III) sulfate (Table 4, Figure 4), while ferrihydrite (a low crystalline iron oxide) is the dominant species for all other surrogates (Table 4, Figure 4). All surrogates except MM contained similar amounts of iron oxide (20–30%); the remaining iron either formed ferrihydrite (<70%) or iron sulfate (<70%, Table 4). This is significant, as the surface exposed iron is typically hydroxylated, while bulk and unexposed iron would have the form of iron oxide. The lack of Fe availability (iron hydroxide) in BMMS and PMMS corresponds to the significant decrease of EPFRs in these surrogates.

The surface characterization using XPS showed higher zinc concentrations for BMMS and PMMS compared to BMMCaS and PMMCaS (SI Figure S3). The same cannot be confirmed for iron as it was not detected at the surface by XPS for any sample (MWI, MEDWI, and all surrogates). However, the detection of zinc on the surface of BMMS and PMMS further confirms metal availability for EPFR formation.

On the basis of this information we have concluded that the suppression mechanism of EPFR formation is associated with the adsorption of SO_2 to the surface metal sites. Once reacted, surface sulfates are formed, deactivating the metal centers toward the adsorption of organic precursors and thus formation of EPFRs.

Environmental Relevance

The formation of predominantly metal sulfate in the surrogates containing only sulfur (BMMS and PMMS), predominantly calcium sulfate in the surrogates containing both calcium and sulfur (BMMCaS and PMMCaS), and associated changes of EPFR formation propensity indicate the different chemical behavior of the applied agents (S, Ca), depending on if they are introduced together or not. In particular, it is evident that the SOx formed during the calcination of the surrogate samples (decomposition of ammonium sulfate) binds to the metal oxides, effectively blocking part of the potential sites for EPFR formation. However, if calcium is present in the system, then calcium sulfate is formed preferentially.

The beneficial activity on the prevention of EPFR formation and potentially on PCDD/F emissions should be considered as a measure to control the emissions. Present studies suggest that SOx scrubbing from combustion systems should probably be moved to a lower temperature range to allow for reactions between the metal oxides in active surfaces with SO_2. This can potentially limit the formation of EPFRs and PCDD/Fs down the exhaust stream. Engineering a way to apply this presented method to incineration and hazardous waste sites (i.e., Superfund sites) will be innovative and beneficial to the environmental health community.

Acknowledgments

Funding

NIEHS Grant 2P42ES013648.

The authors would like to thank the NIEHS Grant 2P42ES013648 for funding this project. The authors would also like to thank Paul Lemieux and Shenyong Lu for their contribution of fly ashes from incinerators for these studies. Lastly, the authors would like to thank Amitava Roy at CAMD for his assistance in understanding synchrotron techniques.

References

1. Balakrishna S, Lomnicki S, McAvey KM, Cole RB, Dellinger B, Cormier SA. Environmentally persistent free radicals amplify ultrafine particle mediated cellular oxidative stress and cytotoxicity. Part Fibre Toxicol. 2009; 6 doi:1110.1186/1743-8977-6-11.
2. Cormier SA, Lomnicki S, Backes W, Dellinger B. Origin and health impacts of emissions of toxic by-products and fine particles from combustion and thermal treatment of hazardous wastes and materials. Environ Health Persp. 2006; 114(6):810–817.
3. Dellinger B, Lomnicki S, Khachatryan L, Maskos Z, Hall RW, Adounkpe J, McFerrin C, Truong H. Formation and stabilization of persistent free radicals. Proc Combust Inst. 2007; 31:521–528. [PubMed: 25598747]
4. Balakrishna S, Saravia J, Thevenot P, Ahlert T, Lominiki S, Dellinger B, Cormier SA. Environmentally persistent free radicals induce airway hyperresponsiveness in neonatal rat lungs. Part Fibre Toxicol. 2011; 8 doi:1110.1186/1743-8977-8-11.
5. Lomnicki S, Truong H, Vejerano E, Dellinger B. Copper oxide-based model of persistent free radical formation on combustion-derived particulate matter. Environ Sci Technol. 2008; 42(13): 4982–4988. [PubMed: 18678037]
6. Vejerano E, Lomnicki S, Dellinger B. Formation and Stabilization of Combustion-Generated Environmentally Persistent Free Radicals on an Fe(III)(2)O-3/Silica Surface. Environ Sci Technol. 2011; 45(2):589–594. [PubMed: 21138295]
7. Vejerano E, Lomnicki SM, Dellinger B. Formation and Stabilization of Combustion-Generated, Environmentally Persistent Radicals on Ni(II)O Supported on a Silica Surface. Environ Sci Technol. 2012; 46(17):9406–9411. [PubMed: 22831558]
8. Dellinger B, Truong H, Wu H, Lomnicki S, McCarley R, Poliakoff ED. Combustion-generated nanoparticles: The role of transition metals in pollutant formation. Prepr Symp - Am Chem Soc, Div Fuel Chem. 2006; 51(1):245–247.
9. Fahmy B, Ding L, You D, Lomnicki S, Dellinger B, Cormier SA. In vitro and in vivo assessment of pulmonary risk associated with exposure to combustion generated fine particles. Environ Toxicol Pharmacol. 2010; 29(2):173–182. [PubMed: 20369027]
10. Varner, KJ., Mahne, S., Chuang, G., Pankey, E., Kuiri, L., Dellinger, B. In Environmentally Persistent Free Radicals Decrease Cardiac Function In Vivo. American Chemical Society; Washington, DC: 2012. p. SWRM–413

11. Freeman LR, Zhang L, Nair A, Dasuri K, Francis J, Fernandez-Kim SO, Bruce-Keller AJ, Keller JN. Obesity increases cerebrocortical reactive oxygen species and impairs brain function. Free Radical Biol Med. 2013; 56:226–233. [PubMed: 23116605]
12. Saravia J, Lee GI, Lomnicki S, Dellinger B, Cormier SA. Particulate matter containing environmentally persistent free radicals and adverse infant respiratory health effects: a review. J Biochem Mol Toxicol. 2013; 27(1):56–68. [PubMed: 23281110]
13. Wang P, Thevenot P, Saravia J, Ahlert T, Cormier SA. Radical-containing particles activate dendritic cells and enhance Th17 inflammation in a mouse model of asthma. Am J Respir Cell Mol Biol. 2011; 45(5):977–983. [PubMed: 21493781]
14. Truong H, Lomnicki S, Dellinger B. Potential for Misidentification of Environmentally Persistent Free Radicals as Molecular Pollutants in Particulate Matter. Environ Sci Technol. 2010; 44(6): 1933–1939. [PubMed: 20155937]
15. Dellinger, HB. In Dioxins, Nanoparticles, Environmentally Persistent Free Radicals and Combustion-Generated Air Pollution. American Chemical Society; Washington, DC: 2008. p. PRES–001
16. Balakrishna S, Fahmy B, Lomnicki S, Dellinger B, Ahlert T, You D, Cormier SA. ANYL 338-Combustion generated nanoparticles: Pro-inflammatory effects and role of oxidative stress in neonatal rat exposure models. Abstracts of Papers of the American Chemical Society. 2008:236.
17. Balakrishna S, Lomnicki S, Dellinger B, Cormier SA. Resveratrol Ameliorates the Redox Imbalances in Human Airway Epithelial Cells Exposed to Combustion Generated Nanoparticles. Free Radical Bio Med. 2008; 45:S44–S44.
18. Dugas TR, Hebert VY, Dellinger B, Lomnicki S, Cormier SA, Varner KJ. Environmentally Persistent Free Radicals are Redox Active and More Cytotoxic than the Average Ultrafine Particle. Free Radical Bio Med. 2009; 47:S121–S121.
19. Fahmy B, Ding L, You D, Lomnicki S, Dellinger B, Cormier SA. In vitro and in vivo assessment of pulmonary risk associated with exposure to combustion generated fine particles. Environ Toxicol Pharmacol. 2010; 29(2):173–182. [PubMed: 20369027]
20. Kelley MA, Thibeaux T, Hebert VY, Cormier SA, Lomnicki S, Dellinger B, Dugas TR. Model Particulate Matter Containing Persistent Free Radicals Exhibit Reactive Oxygen Species Production. Free Radical Biol Med. 2011; 51:S134–S134.
21. Thevenot PT, Saravia J, Jin N, Giaimo JD, Chustz RE, Mahne S, Kelley MA, Hebert VY, Dellinger B, Dugas TR, Demayo FJ, Cormier SA. Radical-Containing Ultrafine Particulate Matter Initiates Epithelial-to-Mesenchymal Transitions in Airway Epithelial Cells. Am J Respir Cell Mol Biol. 2013; 48(2):188–97. [PubMed: 23087054]
22. Thibodeaux, CA., Poliakoff, ED. In Chemisorption of Phenol on fumed Silica and Alumina Supported Cu(II)O Nanoclusters. American Chemical Society; Washington, DC: 2012. p. SWRM–362
23. Kiruri L, Khachatryan L, Lomnicki S, Dellinger B. Effect of Copper Oxide Concentration on the Formation and Persistency of Environmentally Persistent Free Radicals (EPFRs) in Particulates. Environ Sci Technol. 2014; 48:2212–2217. [PubMed: 24437381]
24. Dellinger, B., Lomnicki, S. In Sources and Characterization of Environmentally Persistent Free Radicals. American Chemical Society; Washington, DC: 2008. p. WRM–032
25. dela Cruz ALN, Gehling W, Lomnicki S, Cook R, Dellinger B. Detection of Environmentally Persistent Free Radicals at a Superfund Wood Treating Site. Environ Sci Technol. 2011; 45(15): 6356–6365. [PubMed: 21732664]
26. Dellinger B, Khachatryan L, Masko S, Lomnicki S. Free Radicals in Tobacco Smoke. Mini-Rev Org Chem. 2011; 8(4):427–433.
27. Mekki A, Holland D, McConville CF, Salim M. An XPS study of iron sodium silicate glass surfaces. J Non-Cryst Solids. 1996; 208(3):267–276.
28. Grosvenor AP, Kobe BA, Biesinger MC, McIntyre NS. Investigation of multiplet splitting of Fe 2p XPS spectra and bonding in iron compounds. Surf Interface Anal. 2004; 36(12):1564–1574.
29. Yamashita T, Hayes P. Analysis of XPS spectra of Fe2+ and Fe3+ ions in oxide materials. Appl Surf Sci. 2008; 254(8):2441–2449.

30. Zhang J, Cui H, Wang B, Li C, Zhai J, Li Q. Fly ash Cenospheres supported visible-light-driven BiVO4 photocatalyst: Synthesis, characterization and photocatalytic application. Chem Eng J (Amsterdam, Neth). 2013; 223:737–746.
31. Hormes J, Scott JD, Suller VP. Facility Update: The Center for Advanced Microstructures and Devices: A Status Report. Synchrotron Radiat News. 2006; 19(1):27–30.
32. Ravel B, Newville M. ATHENA, ARTEMIS, HEPHAESTUS: data analysis for X-ray absorption spectroscopy using IFEFFIT. J Synchrotron Radiat. 2005; 12:537–541. [PubMed: 15968136]
33. Kelly, SD., Hesterberg, D., Ravel, B. Analysis of Soils and Minerals Using X-ray Absorption Spectroscopy. Soil Science Society of America; Madison, WI: 2008.
34. Bolton, JR., Weil, JA. Electron Spin Resonance: Elemental Theory and Practical Applications. Chapman and Hall/McGraw-Hill; New York: 1986. p. 497
35. Vejerano E, Lomnicki S, Dellinger B. Lifetime of combustion-generated environmentally persistent free radicals on Zn(II)O and other transition metal oxides. J Environ Monit. 2012; 14(10):2803–2806. [PubMed: 22990982]
36. Mao D, Edwards JR, Kuznetsov AV, Srivastava R. Particle flow, mixing, and chemical reaction in circulating fluidized bed absorbers. Chem Eng Sci. 2002; 57(15):3107–3117.
37. Hopkins M, Muoh O. Predicting PAC, hydrated lime, and trona injection effectiveness in flue gas systems using CFD and physical flow analyses for optimized nozzle design. Int Technol Conf Clean Coal Fuel Syst. 2010; 35:1396–1407.
38. Quispe D, Perez-Lopez R, Acero P, Ayora C, Nieto JM, Tucoulou R. Formation of a hardpan in the co-disposal of fly ash and sulfide mine tailings and its influence on the generation of acid mine drainage. Chem Geol. 2013; 355:45–55.
39. Che Y, Wang Z, Zhou J. Flue gas conditioning by in situ oxidation of SO2 applying dielectric barrier discharge. Asia-Pac J Chem Eng. 2013; 8(5):636–644.
40. Raghunathan K, Gullett BK. Role of Sulfur in Reducing PCDD and PCDF Formation. Environ Sci Technol. 1996; 30(6):1827–1834.
41. Lomnicki S, Dellinger B. Formation of PCDD/F from 2-chlorophenol catalyzed by CuO in combustion exhaust. Abstracts of Papers of the American Chemical Society. 2003; 225:U819–U819.
42. Nganai S, Lomnicki S, Dellinger B. Ferric Oxide Mediated Formation of PCDD/Fs from 2-Monochlorophenol. Environ Sci Technol. 2009; 43(2):368–373. [PubMed: 19238966]
43. Nganai S, Lomnicki SM, Dellinger B. Formation of PCDD/Fs from the Copper Oxide-Mediated Pyrolysis and Oxidation of 1,2-Dichlorobenzene. Environ Sci Technol. 2011; 45(3):1034–1040. [PubMed: 21174454]
44. Ordóñez S, Paredes JR, Díez FV. Sulphur poisoning of transition metal oxides used as catalysts for methane combustion. Appl Catal, A. 2008; 341(1–2):174–180.
45. Kurt M, Say Z, Ercan KE, Vovk EI, Kim CH, Ozensoy E. Sulfur Poisoning and Regeneration Behavior of Perovskite-Based NO Oxidation Catalysts. Top Catal. 2017; 60:40–51.
46. Knapp GS, Veal BW, Pan HK, Klippert T. XANES study of 3d oxides: Dependence on crystal structure. Solid State Commun. 1982; 44(9):1343–1345.

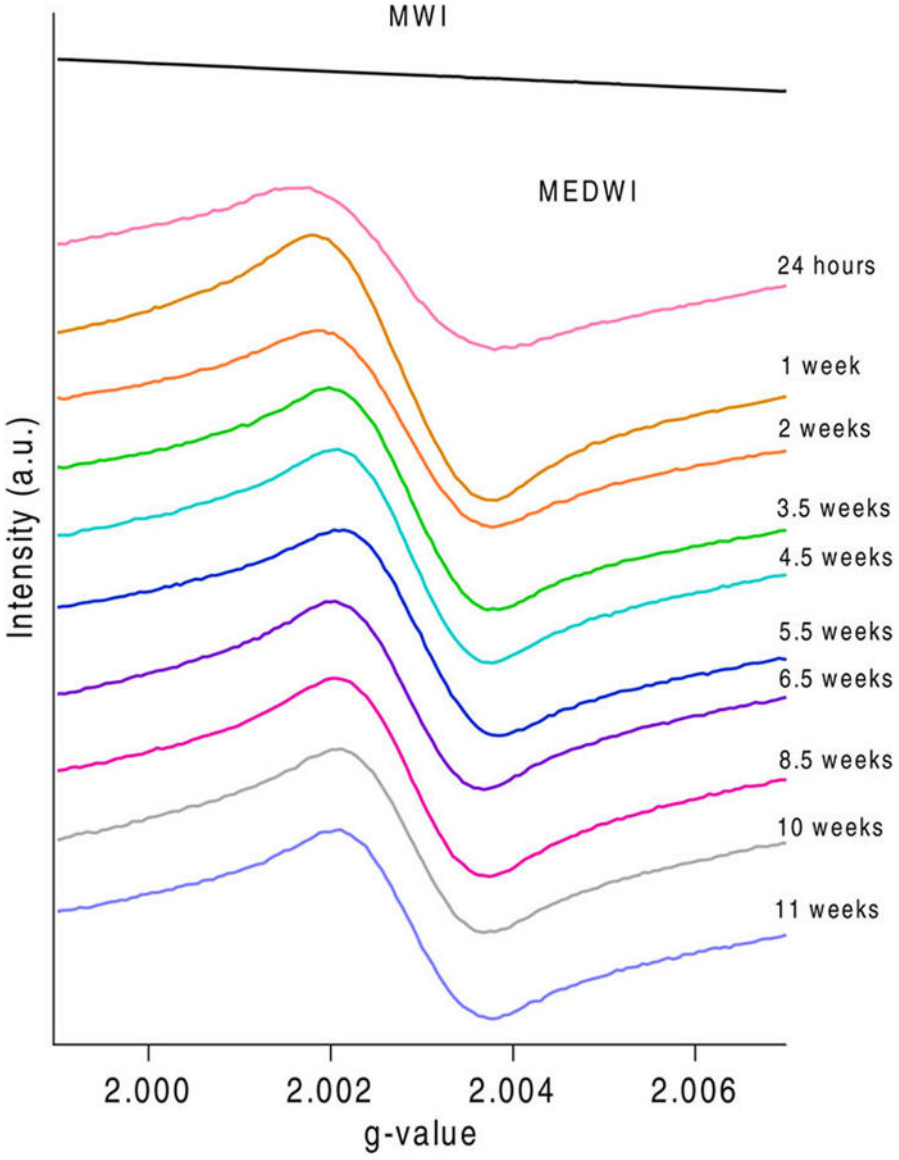

Figure 1.
EPFR species formation difference for MWI and MEDWI of varying ages.

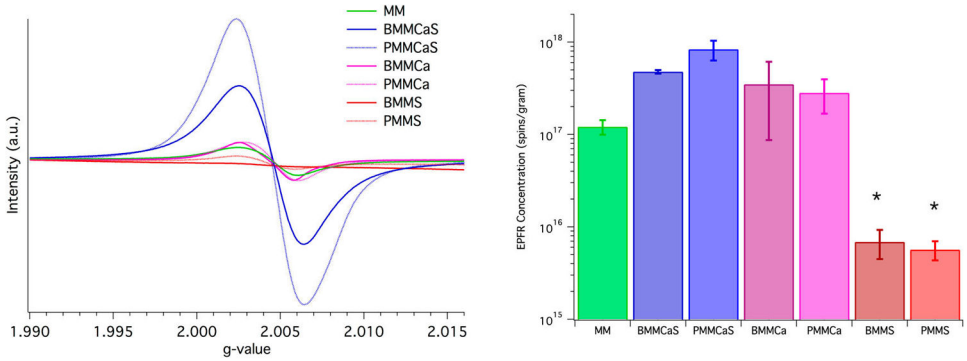

Figure 2.

EPR spectra (left) and resulting plot of EPFR concentration (right) for all surrogates. Note the significant difference between surrogates with only sulfur (*−$p < 0.05$).

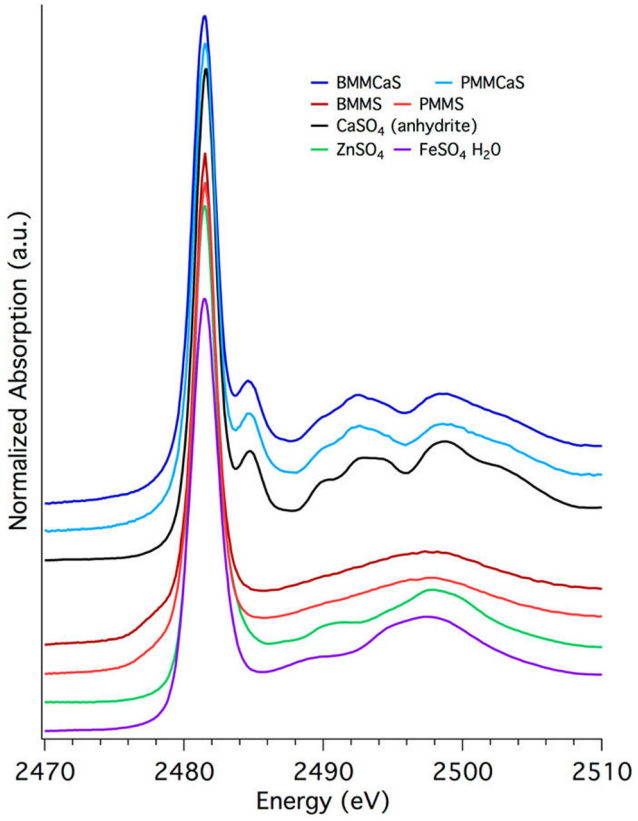

Figure 3.
S K-edge XANES spectra for surrogates containing sulfur.

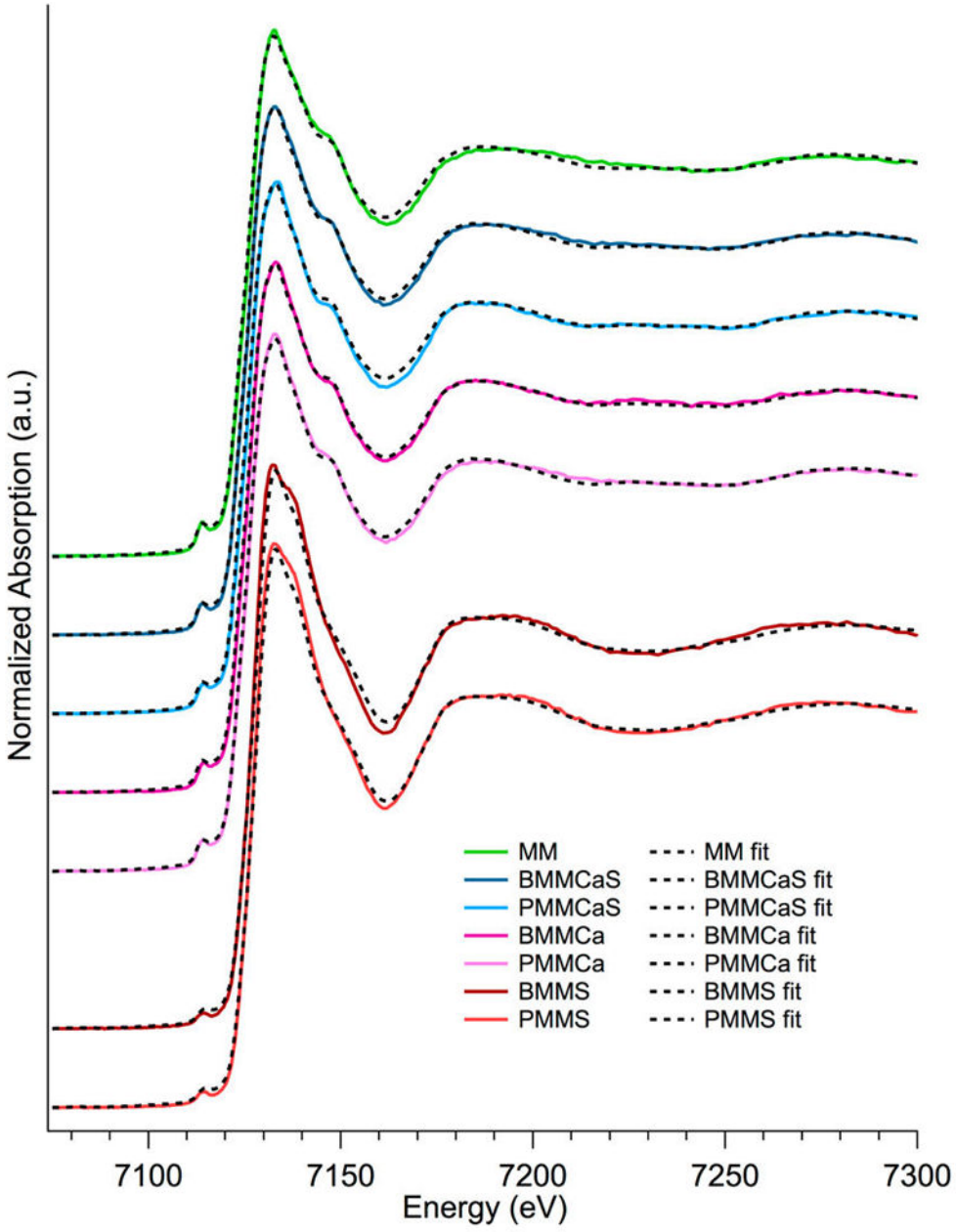

Figure 4.
Fe K-edge XANES and LCF spectra of surrogate samples.

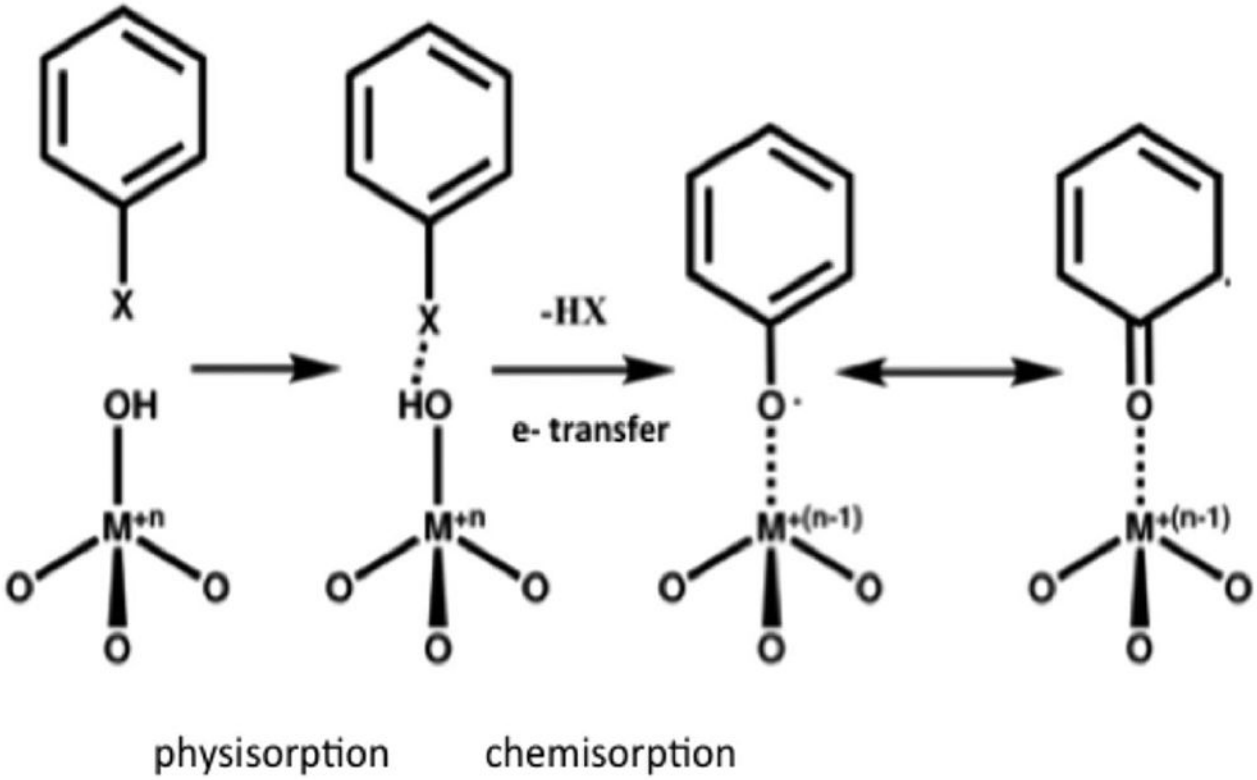

Scheme 1.

EPFR Formation between Organics and Transition Metals (Figure Adapted from Balakrishna, S. et. al., 2009)[1]

Table 1

Order of Introduction of Elemental Components into Surrogate Fly Ashes and Respective Naming Notation of the Samples

surrogate	mixed metals (MM)	BMMCaS	PMMCaS	BMMCa	PMMCa	BMMS	PMMS
before- calcination	MM	MM, Ca, S	MM	MM, Ca	MM	MM, S	MM
post- calcination			Ca, S		Ca		S

Table 2

ICP Data of Real World Fly Ashes in % w/w

	Ca	Fe	Mg	P	S	Ti	Zn
MWI	8.6–25	0.9–4.0	1.3–2.0	0.3–1.3	1.3–3.4	0.3–0.8	0.3–0.7
MEDWI	10–11	0.2	1.0	2.3	0.3	0.0	4.3–6.5

Table 3

XPS Based Surface Composition of MEDWI and MWI Fly Ashes in Atomic %

	Mg	Si	P	S	Cl	C	K	Ca	O	Zn	Na
MWI	0–3.7	0–5.3	0	0–8.7	7.1–35.3	15.6–33.7	0–8.5	10.1–16.5	30.7–41.9	0	0–1.8
MEDWI	0	0–6.6	0–0.4	0	0	71.5–82.1	0	0	16.6–21.4	0.5–0.7	0

Environ Sci Technol. Author manuscript; available in PMC 2018 March 19.

Table 4

LCF Results of XANES Spectra at the Fe K-Edge in %

	MM	BMMCaS	PMMCaS	BMMCa	PMMCa	BMMS	PMMS
FeO	0	0	0	0	0	0	0
$FeSO_4$	0	0	0	0	0	0	0
$Fe_2(SO_4)_3$	0	0	0	0	0	71	74
Fe_5HO_8	100	80	75	77	70	0	0
$FeCO_3$	0	0	0	0	0	0	0
Fe_2O_3	0	20	25	23	30	28	26